

Structure studies of exotic nuclei using (p,p') reactions

V. Lapoux,^{1,*} N. Alamanos,¹ and E. Khan²

¹*CEA-SACLAY, DSM/DAPNIA/SPhN 91191 Gif-sur-Yvette, FRANCE*

²*IPN-Orsay, IN2P3-CNRS, 91406 Orsay Cedex, FRANCE*

The structure of the radioactive beams is investigated using the simplest possible probe : the proton used as a target in inverse kinematic reactions. From (p,p') reactions, information on the neutron and proton transition densities is obtained through the comparison between the measured inelastic cross sections to the ones calculated using a microscopic potential and theoretical densities. (p,p') inelastic scattering data to the first excited state for the halo nucleus ${}^6\text{He}$ and for other nuclei ${}^{34}\text{Ar}$ and ${}^{34,36}\text{S}$ have been measured at GANIL using the MUST telescopes. This allows to extract the global features of the transition densities, as shown for the halo nucleus ${}^6\text{He}$. We can also probe the evolution of the shell structure along isotopic chains as moving towards the neutron or proton drip-lines. The example of the sulfur isotopic chain is discussed.

I. MOTIVATIONS FOR STRUCTURE STUDIES

We perform structure studies using (p,p') reactions. Our aim is to obtain the spatial repartition of the nucleons of exotic nuclei, namely the densities, ground state and transition densities to excited states. The observables for the structure studies are angular cross sections of elastic and inelastic scattering.

Nuclear structure of stable nuclei is obtained through electron scattering experiment and this gives charge then proton densities by unfolding the proton distribution. With electrons, we rely on the very well known electromagnetic interaction to obtain the repartition of the protons. The neutron densities were deduced by using hadronic probes : proton, alpha, pions. Far from the valley of stability, the species are short-lived radioactive nuclei and cannot form targets so we rely on the simplest probe, protons, used as target in inverse kinematics

*vlapoux@cea.fr

experiments. Proton elastic scattering is a well-known tool for the study of ground state densities, since the interaction potential can be related to the ground state nuclear densities. In the case of radioactive nuclei, the interpretation of the data is complex, since we are dealing with nuclei having low threshold energies. They can easily couple to excited states or to continuum states during their interaction with a target, and the theoretical difficulty is to calculate the couplings accurately, to extract unambiguously information on the structure. Experimentally the difficulty is to work with radioactive beams having lower and lower intensities as moving towards the driplines. With high statistics, if a large transfer momentum is covered, it is possible to extract accurately from (p,p') data the radial structure of the nucleus as was done in the case of ^{18}O in Ref. [1]. For radioactive beams, generally the poor statistics do not allow to give precisely the ground state and transition densities as a function of the radial coordinate. Nevertheless, the (p,p') are a good tool to constrain the structure models proposed for the exotic nuclei : from (p,p') we can deduce the features of the transition densities allowing to reproduce the data and compare them to the theoretical ones. During the last fifteen years, elastic and inelastic scattering direct reactions like Coulomb excitation (Coulx) and (p,p') were performed with the radioactive beams to learn about the proton and neutron transition densities. Different scenari including core polarization mechanisms, neutron and proton interaction with the core can be evoked to describe these transition densities. It is possible to know if we need a change in the description of the shells, deformation in neutron and proton densities, large enhancement in proton and neutron transition probabilities.

For instance, in the case of light neutron-rich nuclei, we can test densities with neutron halo or skin developing "exotic" forms, compared to the stable nuclei. The halo is a direct consequence of the weak binding energies of the valence nucleons : in the case of ^6He , the 2 neutron separation energy is small, 975 keV, which allows the wave functions to extend far from the core potential [2, 3]. These exotic nuclei are changing the normal rules of our text books of nuclear physics. Sizes are different from what is expected from the short range of the nuclear force and correlations play an important role [4], the decay to cluster states is favoured, proton and neutron may behave differently (see the report on neutron-rich Boron isotopes by W. von Oertzen in this book [5]), and magicity may disappear.

By (p,p') we can probe the structure and test the prediction of models (either cluster or mean field models) for the densities. Our tool to analyze the data is a microscopic potential

which is introduced in the following section.

II. ANALYSIS OF (P,P') REACTIONS USING THE MICROSCOPIC POTENTIAL

A. The microscopic JLM potential

The nucleus-nucleon interaction for the elastic scattering on protons is taken as the microscopic, complex and parameter-free JLM (Jeukenne, Lejeune, Mahaux, from the authors' names) potential [6]. This potential is based upon infinite matter calculations, and it is built on the Reid hard-core Nucleon-Nucleon (NN interaction, using the Brueckner-Hartree-Fock approximation. An improved Local Density Approximation is applied to derive the potential in the case of a finite-range nucleus of density ρ , neutron and proton densities ρ_n and ρ_p . The complex local JLM potential depends only on incident energy E and on ρ_p , ρ_n . The JLM potential was parameterized for incident energies $E \leq 160$ MeV. In general, it is written using λ_V and λ_W the normalization factors for the real and imaginary parts :

$$U_{JLM}(\rho, E)(r) = \lambda_V V(\rho, E)(r) + i\lambda_W W(\rho, E)(r) \quad (1)$$

In general, (for $A \geq 20$) λ_V and λ_W can be slightly modified (less than 10%) to fit the nucleus-nucleon data, but they are close to 1 for all $A \geq 20$ stable nuclei. It was shown that usually in the case of light nuclei ($A \leq 20$) $\lambda_W = 0.8$ [7]. We adopt it as the standard normalization of JLM for light nuclei. This potential allows a good reproduction of large sets of nucleon-nucleus data [7–9]. The Fig. 1 shows it in the case of the light stable nucleus ^{16}O . The potential is calculated using a 2 parameter-Fermi (2pF) density for ^{16}O . The parameters of the 2pF proton density are fitted on the density extracted from the electron scattering.

The inelastic (p,p') angular cross sections are obtained through Distorted Wave Born approximation (DWBA) calculations including the JLM potential. They are performed with the TAMURA code [10]. The entrance, transition and exit channel potentials are defined with the ground state and transition density. The normalization of the real and imaginary parts is fixed with the values obtained in the analysis of the elastic scattering. For a J_i to J_f transition the density is written : $\rho^{tr} = \langle \Psi_f | \delta(\vec{r} - \vec{r}^j) | \Psi_i \rangle$. The calculated inelastic (p,p') cross sections are sensitive to M_n and M_p factor, which are the radial moments of the

transition densities :

$$M_{p,n} = \int dr r^{l+2} \rho_{p,n}^{tr}, \quad (2)$$

with l the multipolarity of the transition. These factors can also be expressed as the matrix elements of the electromagnetic multipole operators $O_{p(n)}^l$ between nuclear states [11], l being the multipolarity of the transition :

$$M_{p,n} = \langle J_f T T_z | O_{p(n)}^l | J_i T T_z \rangle \quad (3)$$

The M_p factor is directly related to the $B(E_l)$ transition strength value obtained by Coulex experiment. We adopt here the following convention for the relationship between $|M_p|$ and $B(E_l)$:

$$B(E_l, J_i \rightarrow J_f) = \frac{(2J_f + 1)}{(2J_i + 1)} |M_p|^2 \quad (4)$$

The models of elastic and inelastic scattering on proton including the potential JLM were proven to be reliable to extract the fundamental quantities such as M_n/M_p without ambiguity for the stable nuclei [8] as well as for the exotic nuclei [9, 12]. $M_{n,p}$ can be used as a signature for the modification of the shell structure and compared to the values predicted by different structure models.

A simple analysis of the (p,p') can be performed using the phenomenological Tassie form [13] for the densities. The proton (p) or neutron (n) transition density is obtained by derivating the ground state density

$$\rho_{p(n)}^{tr,l}(r) = -\alpha_{p(n)}^l r^{l-1} \frac{d\rho_{p(n)}}{dr} \quad (5)$$

The proton density is normalized with the α_p^l by requiring that its moment $|M_p|$ should satisfy the Eq. 4 with $B(E_2)$ obtained by Coulex. $|M_n|$ is then deduced by adjusting calculated (p,p') on the data.

B. Role played by the coupling to the continuum in the elastic scattering : the ${}^6\text{He}$ + p entrance channel

For the analysis of direct reactions we need the potential of the entrance channel, namely the potential deduced from the elastic scattering. To study the effect of the weak binding on the interaction potential between a light exotic nucleus and a target, elastic scattering cross sections of the ${}^6\text{He}$ secondary beam, at 38.3 MeV/nucleon, on proton have been measured

at GANIL. The ${}^6\text{He} + \text{p}$ results, as well as other existing data, are analyzed within the framework of the microscopic JLM potential [6]. A halo-type density given by few-body model calculations [14], with a matter root mean square (rms) radius of 2.55 fm was used to generate the potential. The rms value of this density corresponds to the value obtained by few-body analysis [15] of the high-energy ${}^6\text{He} + \text{p}$ elastic scattering [16]. We have shown [17, 18] that the angular distributions of ${}^6\text{He}$ on proton are better reproduced with a reduction of the real part of the JLM optical potential as seen in Fig. 2. The origin of this effect was discussed in Ref. [19] and may be explained within the theory developed by Feshbach [20]. According to this theory, the interaction potential should be written as $U = V + U_{pol}$ where V is the usual real potential and U_{pol} is the dynamical polarization potential (DPP). V can be seen as the folding potential or the elastic potential described by microscopic or phenomenological models. It includes only the interaction between the projectile and the target ground states. The DPP is complex, non-local and energy-dependent, it arises from couplings to inelastic channels. For well-bound nuclei, the probability to excite during the elastic scattering is weak, and the main contribution is imaginary, represented by the usual phenomenological imaginary part W . For weakly-bound nuclei, the particle threshold is close to their ground state, which favours couplings to the excited states and to the continuum during their interaction with a target. This leads to a greater influence of the DPP and then to the reduction of the real part of the nuclear potential [21]. Therefore, one must take into account in the analysis the interaction potential term due to transitions going to the excited states and then back to the ground state [19]. However the precise calculation of the DPP requires the knowledge of the spectroscopy of the nucleus and also the knowledge of low-lying resonant states and couplings to the continuum. The scheme for such a transition occurring during the elastic scattering is presented in Fig.3. It was explained in Ref. [21, 22] that a complex surface potential, with a repulsive real part, is expected to simulate the surface effects generated by the polarization potential and this corresponds to the reduction of the real part [17]. This effect is observed in the ${}^6\text{He} + \text{p}$ scattering, analyzed with the JLM potential [18] and shown in Fig. 2. By taking it into account in the JLM calculation, we have reproduced successfully the data at 38.3 MeV/nucleon together with other data for ${}^6\text{He}$ on proton, measured at Riken [23] at $E/A = 71$ MeV and at Dubna [24] at $E/A = 25$ MeV. The whole set of data is compared to the calculations in Fig. 2 [18].

Recently the structure of the halo nucleus ${}^6\text{He}$ was explored through proton inelastic

(p,p')scattering [25]. The interaction potential tested on the elastic scattering will be used in the calculation of the (p,p') scattering.

C. Experimental setup

For (p,p') reactions, the experimental apparatus MUST [26], an array of three-stage telescopes (a set of Si-strips, SiLi and CsI telescopes) specifically designed to detect recoiling light charged particles, is used to measure angular distributions for elastic and inelastic scattering of radioactive beams on proton target. Using MUST, (p,p') scattering data to the first excited state of ${}^6\text{He}$ at 1.8 MeV were measured with a 40.9 MeV/nucleon ${}^6\text{He}$ beam produced at GANIL [25]. The MUST detector has detected the recoil proton in coincidence with a plastic scintillator measuring the heavy nucleus focused at forward angle. The profile of the incident beam was given by two multi-wire chambers, CATS [27], developed by the DAPNIA/SED. Energy, time of flight (between MUST and CATS) and position of the light charged particle are measured in the MUST detector, allowing for a full reconstruction of the (p,p') kinematics. Inelastic scattering on proton, to the first excited states, below the proton separation threshold, for the nuclei ${}^{10,11}\text{C}$, were also measured at $E_{lab} \simeq 40$ MeV/nucleon using the MUST device. A sketch of the experimental device can be found in Ref. [28] and a description of the analysis performed in this case.

By (p,p') we can probe the structure and test the prediction of models (either cluster or mean field models) for the densities.

III. DISCUSSION OF THE ${}^6\text{HE}(P,P')$ REACTION

(p,p') scattering data to the first excited state of ${}^6\text{He}$ at 1.8 MeV have been measured at GANIL with the MUST telescopes. The results obtained at 40.9 MeV/nucleon [25] allows to test different shapes for the transition densities. Here we test two options for the ground state and transition densities included in the JLM potential : one corresponding to a non-halo case, with a matter rms radius equal to 2.2 fm, the other one having the features of a halo density, namely the large extension of the neutron density, and a larger matter rms radius of 2.5 fm. The transition densities are derived from ground state densities by applying the Tassie model as was explained in Sec. II A. The calculations of

the (p,p') cross sections for these two options are compared with the experimental data. We renormalized the theoretical proton transition in order to obtain a $B(E2)$ corresponding to the experimental value ($3.1 \pm 0.6 e^2 \cdot \text{fm}^4$) given in Ref. [29]. The M_p value given by Eq. 4 is equal 0.79 fm^2 . To reproduce the (p,p') data, we have to renormalize the neutron densities given by the Tassie model, and this corresponds to M_n/M_p equal to 4.4 or to 2.7 for the halo and non-halo cases for the densities, respectively. In Fig. 4, the dashed and solid curves correspond to the “non-halo” and “halo” options, respectively. The ${}^6\text{He}(p,p')$ analysis using JLM is in favour with the halo configuration for this nucleus. Here we can provide a realistic shape for the neutron and proton gs and transition densities, that can be easily compared to the structure for ${}^6\text{He}$ predicted theoretically. A precise analysis including directly the effects of the couplings to the continuum was done using the CDCC Coupled-channel calculations and a dineutron model for ${}^6\text{He}$ [30]. It was applied to the ${}^6\text{He}+p$ elastic, inelastic and transfer data measured at Dubna. It helps in determining the influence of the DPP. Nevertheless, through optical model calculations based on the JLM model, we directly test the densities. Both approaches are complementary : the CDCC to fix the couplings, JLM model to extract the densities.

${}^{10,11}\text{C}(p,p')$ scattering data were also measured using the MUST detectors. These nuclei, like the other carbon isotopes described in the theory of the Antisymmetrized Molecular Dynamics (AMD) [31] are expected to have a proton density with an oblate deformation. The aim of the experiment was to obtain structure information for these two neutron-deficient radioactive nuclei and to compare data to calculations performed with different models predicting the ground state and transition densities. The analysis performed with the JLM potential is explained in these proceedings [28].

IV. EVOLUTION OF THE SULFUR ISOTOPES

The ground state neutron and proton densities are given from HF+ BCS (SGII) calculations using the SGII parameterization of the effective Skyrme interaction. The transition densities are obtained through QRPA calculations with SGII. They are described in Ref. [32].

These calculations are well suited to interpret the excitations in terms of $p - h$ (or two quasiparticles) configurations. To show the validity of the JLM interaction we have per-

formed a test calculation on the stable nucleus ^{32}S using the experimental ground and transition densities $0^+ \rightarrow 2^+$ of ^{32}S . The proton densities are deduced from the charge densities known from (e,e') scattering and we assume that the neutron densities are identical to the proton ones to perform the JLM calculations. The good agreement obtained with the MUST data measured at 53 MeV/nucleon is shown in Fig. 5. For this stable nucleus, no renormalization of the real part is needed, neither of the imaginary part, since we are in this intermediate-mass region. We adopt also for all sulfur isotopes the normalization factor $\lambda_W = 1$. For ^{38}S , the QRPA calculations give a reasonable agreement with the data, as displayed by Fig. 6. As shown in Fig. 7 the trend of the $B(E2)$ values is well reproduced by the QRPA calculations. When crossing the shell gap, the shell closure $N=20$ can be clearly seen as a minimum of the $B(E2)$ values (combined with the increase of the 2^+ excitation energies and decrease of S_{2n} separation energies) For the sulfur isotopes the $N=20$ closure is well seen on the $B(E2)$, and correspondingly in the evolution of the M_p . The trend of the M_n value is also interesting : the evolution of the neutron excitations is close to the one of the protons, which shows collective behaviour of the densities. Proton elastic and inelastic scattering angular distributions to the 2_1^+ and 3_1^- states of ^{34}Ar were measured using the MUST Si strip detector array with a secondary beam produced at Ganil. They are presented in Fig. 8. The agreement is good for the elastic and inelastic scattering to the 2^+ but the angular 3^- angular distributions are overestimated by the calculations. The measurement of the 3^- distributions are a good constraint on the models : we test the treatment of negative parity states in ^{34}Ar , implying p - h excitations across a shell gap. The calculated M_p and M_n values for the Argon isotopes (see Fig. 9) show that the $N=20$ remain a good magic number, but for $N=28$, the decreases of M_n and M_p are less pronounced, indicating a possible weakening of the shell effects. Coulex and (p,p') data are needed for $^{45,46}\text{S}$ and $^{47,48}\text{Ar}$ in order to clarify the picture.

As can be seen in the case of Sulfur and Argon isotopes, extracting the systematic behaviour along isotopic chain from the neutron-deficient to neutron-rich side and combining $B(E2)$ value (i.e. $|M_p|$) and M_n can provide strong constraint on the theoretical shell structure models.

V. PERSPECTIVES USING THE (P,P') TOOL

The next generation facilities are expected to deliver radioactive beams at high intensities allowing to extract precisely the nuclear transition densities, as was done in the past for stable beams [1], by leading model-independent analysis of the (p,p') reactions. At present, we can probe the transition densities predicted by shell model, HFB, QRPA ou cluster-model calculations. Since the elastic potential is the entrance channel of all more complicated direct reactions, like inelastic scattering and transfer reactions, it has to be correctly tuned on the elastic scattering. The measurement of the elastic scattering is required, if a reliable information on structure has to be extracted from inelastic or transfer reactions. In our case, it has allowed to probe the transition densities from the ground to the first excited state of the nuclei ${}^6\text{He}$ and ${}^{10}\text{C}$, and for sulfur and Argon isotopes.

-
- [1] J. Kelly et al., Phys. Rev. C **41** (1990) 41.
- [2] P. G. Hansen and B. Jonson, Europhys. Lett **4**, 409 (1987).
- [3] S. N. Ershov *et al.*, Phys. Rev. C **56**, 1483 (1997).
- [4] Y. Oganessian, *Proceedings of the HIPH02 Conference, Dubna 2002*.
- [5] W. von Oertzen, *Proceedings of the HIPH02 Conference, Dubna 2002*.
- [6] J. P. Jeukenne, A. Lejeune and C. Mahaux, Phys. Rev. C **16**, 80 (1977).
- [7] J. S. Petler *et al.*, Phys. Rev. C **32**, 673 (1985).
- [8] S. Mellema, R. Finlay, F. Dietrich and F. Petrovich, Phys. Rev. C **28**, 2267 (1983).
- [9] N. Alamanos, F. Auger, B. A. Brown and A. Pakou, J. Phys. G **24** (1998) 1541.
- [10] T. Tamura, W. R. Coker, R. Rybicki, Comp. Phys. Commun. **2** (1971)94.
- [11] [A.M. Bernstein, V.R. Brown and V.A. Madsen, Phys. Rev. Lett. **42**, 425 (1979).
- [12] E. Khan *et al.*, Phys. Lett. B. **490** (2000) 45.
- [13] G.R. Satchler, *Direct Nuclear Reactions*, CLARENDON PRESS, Oxford University Press 1983.
- [14] J. Al-Khalili, J. Tostevin and I. Thompson, Phys. Rev. C **54**, 1843 (1996).
- [15] J.S. Al-Khalili and J.A. Tostevin, Phys. Rev. C **57**, 1846 (1998).
- [16] G. D. Alkharov *et al.*, PRL **78**, 2313 (1997).
- [17] V. Lapoux, PhD Thesis, Université d'Orsay, 1998, DAPNIA/SPHN-98-05T.
- [18] V. Lapoux *et al.*, Phys. Lett. B **517**, 18 (2001).
- [19] M.E. Brandan and G. R. Satchler, Phys. Rep. **285**, 143 (1997).
- [20] H. Feshbach, Ann. Phys. **5**, 357 (1958).
- [21] Y. Sakuragi *et al.*, Prog. Th. Phys. **70** 4 (1983) 1047.
- [22] Y. Sakuragi, Phys. Rev C **35**, 2161 (1987).
- [23] A.A. Korshennikov *et al.*, Nucl. Phys. A **617**, 45 (1997).
- [24] R. Wolski *et al.*, Phys. Lett. B **467**, 8 (1999).
- [25] A. Lagoyannis *et al.*, Phys. Lett. B **518**, 27 (2001).
- [26] *The MUST collaboration*, NIM Phys. Res. A **421** (1999) 471-491.
- [27] S. Ottini *et al.*, Nucl. Instr. and Meth. A **431**, 476 (1999).
- [28] C Jouanne *et al.*, *Proceedings of the HIPH02 Conference, Dubna 2002*.

- [29] T. Aumann *et al.*, Phys. Rev. C **59**, 1252 (1999).
- [30] K. Rusek, K. W. Kemper, R. Wolski, PRC **64**, 044602.
- [31] Y. Kanada-En'yo and H. Horiuchi, Phys. Rev. C **55**, 2860 (1997).
- [32] E. Khan *et al.*, NPA **694** (2001) 103-131.

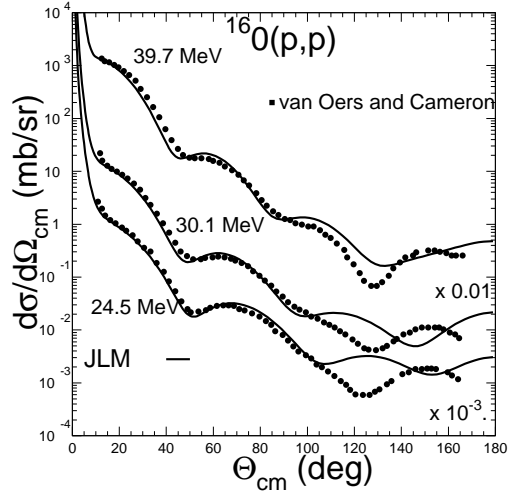


Figure 1: Comparison between experimental data for the proton elastic scattering of ^{16}O and calculations done using the JLM potential and explained in the text.

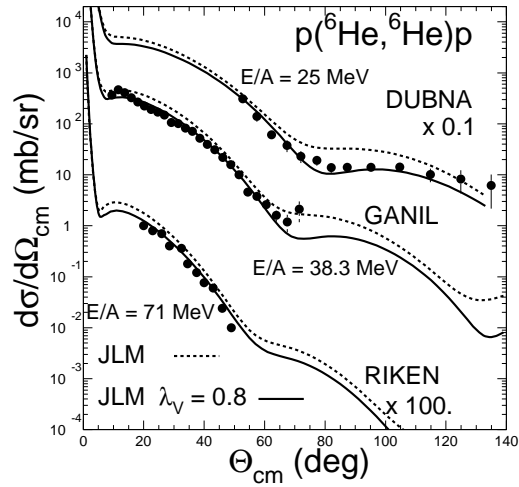


Figure 2: The $^6\text{He}+p$ GANIL data at 38.3 MeV/nucleon are plotted with previous data obtained at Dubna in a first experiment [24] at 25 MeV/nucleon and at Riken [23] at 71 MeV/nucleon. The lines are calculated with the JLM potential (dashed lines). The data are reproduced with a reduction of the real part by a factor 0.8 (solid line).

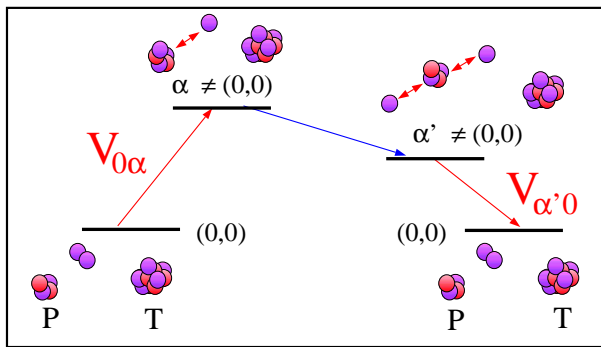


Figure 3: Scheme of the virtual couplings occurring during an elastic scattering between projectile P and target T . They contribute to the DPP term in the total elastic optical potential.

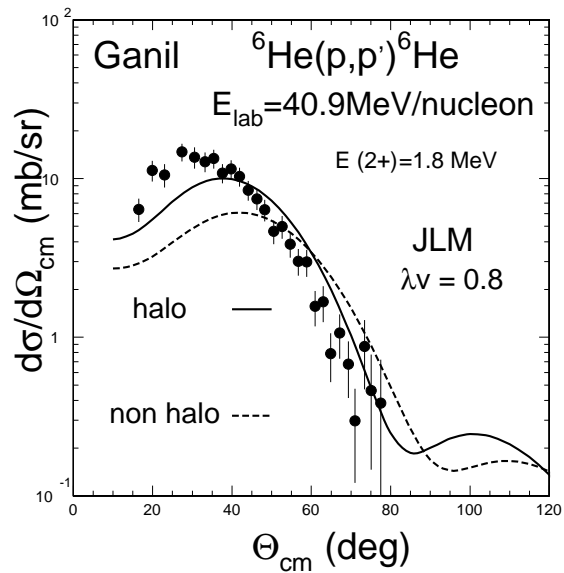


Figure 4: Comparison between data obtained at 40.9 MeV/nucleon using MUST [25] and JLM calculations allowing to test two kinds of phenomenological transition densities based on the Tassie model.

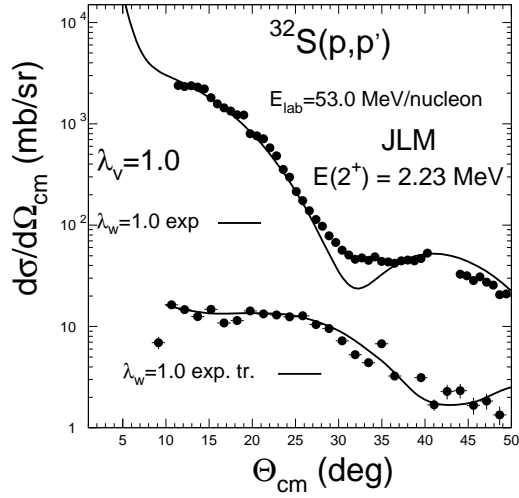


Figure 5: Experimental $^{32}\text{S}(p,p')$ angular distributions measured at 53 MeV/nucleon are compared to calculations performed with the JLM potential and using experimental densities, as described in the text.

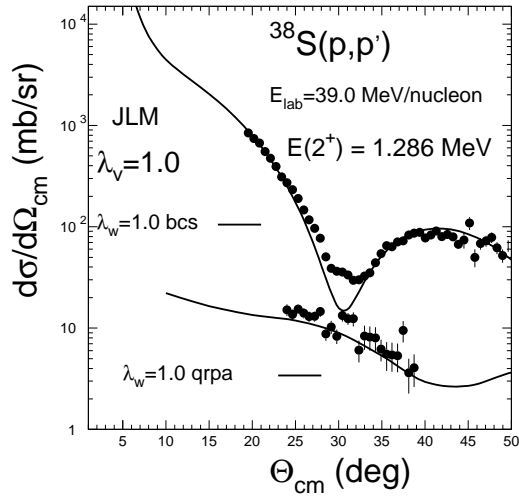


Figure 6: Comparison between JLM calculations and experimental $^{38}\text{S}(p,p')$ elastic and inelastic distributions for the 2_1^+ state. The JLM potential is calculated using the ground state densities obtained with HF+BCS and transition densities from QRPA model.

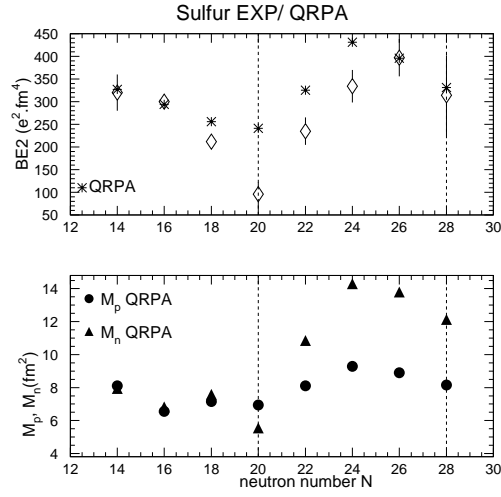


Figure 7: Comparison for Sulfur isotopes between calculated $B(E2)$ values (asterisks) and experimental ones (diamonds) is shown on the top figure, and the M_n and M_p calculated values are displayed below as a function of the neutron number N .

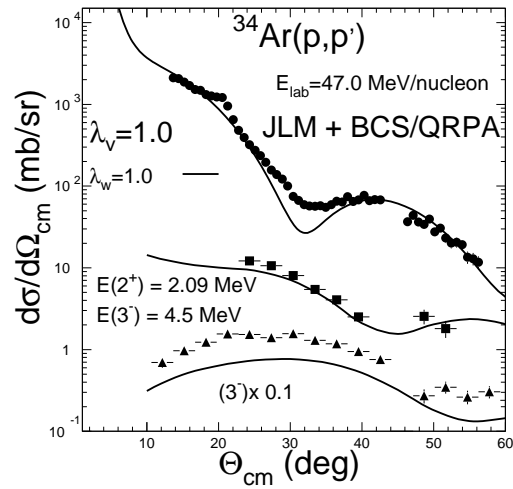


Figure 8: (p,p') ^{34}Ar elastic and inelastic angular distributions for the 2^+ and 3^- states measured at 47 MeV/nucleon. Data are compared with calculations using the JLM potential and densities obtained with HF+BCS and QRPA models.

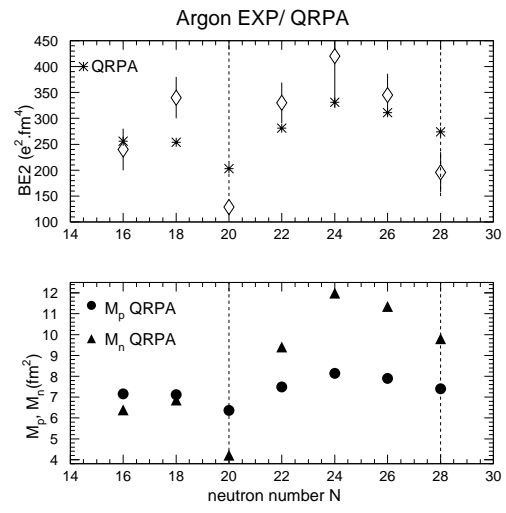


Figure 9: Same as in previous figure but for Argon isotopes.